IEEE Industry Applications Society
Annual Meeting
New Orleans, Louisiana, October 5-9, 1997

Operation of Induction Machines with Electromagnetic Irregularities

Luis Garcés, Russel J. Kerkman, Timothy M. Rowan, Dave Schlegel, Brian J. Seibel, and Kevin Stachowiak
Rockwell Automation - Allen Bradley Company
6400 W. Enterprise Dr.
Mequon WI 53092 USA
Phone (414) 242-8263 Fax (414) 242-8300 E-Mail: rjkerkman@meq1.ra.rockwell.com

Abstract **- The paper presents application data showing an induction motor developing torque at zero slip. This condition can prevent proper field commissioning of the motor drive system and contribute to inferior system performance. The paper examines rotor asymmetries, one cause for the non zero torque condition. Voltage and current spectrums, for current regulated and volts per hertz controllers, are presented. Another source for the non zero torque at zero slip, machine space harmonics, is discussed and analyzed. The paper examines contributions to abnormal machine operation of each source by examining the signals present in the respective waveforms. Control strategies are developed where appropriate to mitigate the adverse effects of the motor irregularities.**

I. INTRODUCTION

Field Oriented (FO) induction motor drives provide a high performance alternative to dc drives and are cost competitive in most applications. State of the art controllers assume the ac machine to be ideal: sinusoidal winding distributions, control parameters reflect a lumped parameter model, saturation of the magnetizing inductance modeled through a lookup table, and may include core loss compensation [1-3].

The above assumptions are necessary for practical FO industrial drives; however, they are simplifications of real machines. Actual machines have stator windings placed in discrete slots, which are open or closed depending if the winding is random or form wound. Discrete slots produce space harmonics and permeance variations, which can produce crawling and cogging. The type of winding also affects machine characteristics. Random wound machines with semi-closed slots exhibit a high power factor, low stray load loss, and a low cost; however, the slot area used is low, end windings are difficult to brace, and the coils require dip and baked varnish to secure the windings, which due to the close proximity of disparate phases lowers the overload capability and life. Form wound stators use more slot area; but they use the iron less effectively, the end winding length is longer making bracing difficult, and terminating the windings to connection blocks is difficult.

Another complicating factor is rotor skew. A rotor is skewed to reduce the effects on performance of the discrete stator and rotor slots. Very beneficial for across the line starting, rotor skewing also benefits adjustable speed drive applications by reducing torque pulsations and cogging at low speed, increasing leakage reactance and reducing current ripple and audible noise. Disadvantages include reduced brake down torque and increased stray load loss.

At first, the above machine design considerations do not appear pertinent to the design of Field Oriented Control (FOC). However, recent literature suggests the influence of second order effects cannot be dismissed [4-6]. For example, motor parameters are not constant with frequency. Skin effect modifies critical machine parameters and limits the effectiveness of commissioning procedures and adaptive controllers [5]. Core loss, another second order effect, alters the torque linearity and in some applications a correction must be implemented. In addition, air gap eccentricities and other mechanical effects adversely influence drive system performance [7].

Finally, the stator/rotor slot combination has preferred ratios, which are normally the result of years of experience with the design of across the line starting applications. However, the application of high performance ac induction motor drives may demand a reexamination of time honored design procedures to allow for more overriding performance requirements.

In this paper, the authors present results of years of application experience, which suggest machine irregularities, inherent in the design, cannot be ignored. Furthermore, the irregularities can result in abnormal machine/drive operation with unacceptable performance in demanding applications.

II. EXPERIMENTAL EVIDENCE OF THE PRESENCE OF UNANTICIPATED ELECTROMAGNETIC TORQUE

No load operation of an induction machine is a well defined state. Ideally the machine's rotor speed in rpm equals the stator excitation frequency divided by pole pairs divided by

07803-4070-1/97/$10.00 (c) 1997 IEEE

sixty. In open loop volts per hertz (V/F) and velocity controlled applications, mechanical loads are accounted for without complication. However, torque controlled applications rely on accurate torque regulation and linearity. In these applications, a drive system producing torque at variance with the design specification is unacceptable.

A. *Torque at Zero Slip: Transient Operation*

Field commissioning of high performance ac drives generally requires a zero speed test, often followed by no load operation at defined speeds to establish the flux profile of the machine. However, a number of anomalies may occur, preventing the convergence of the commissioning procedure. Fig. 1 shows the per unit speed and motor current as a function of time for a 400 hp FO drive system with position feedback. Fig. 2 shows a simplified block diagram of the velocity loop. Although the torque command (Iq) is zero and

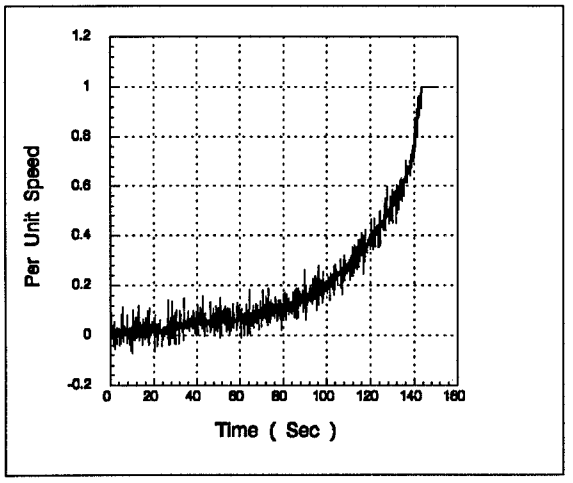

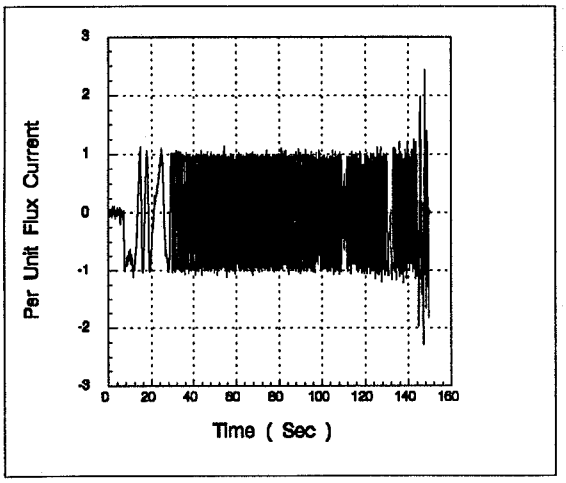

Fig.1 Experimental results flux up acceleration:
speed (upper) 1 pu = 1200 rpm and current (lower) 1 pu =75 Apk.

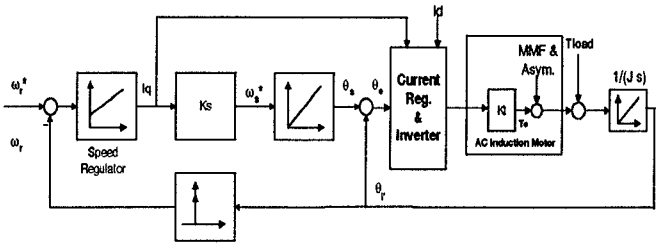

Fig.2 System model.

θs = 0 during flux up, the motor develops an accelerating torque. In fact, as shown in Fig. 1, if left uncontrolled, the motor will accelerate until an overspeed or overcurrent trip occurs. Furthermore, the motor tended to "rock" forward and reverse just before locking in one direction and accelerating. This is clearly evident from the phase reversal in the motor current.

B. *Torque Pulsations at Non-Zero Slip: Steady State Operation*

High performance torque control applications, by necessity, demand accurate torque control, torque regulation, and torque linearity. Torque disturbances originating within the motor-drive require the control to reduce them to acceptable levels. These disturbances if uncorrected will exhibit themselves as velocity disturbances, inferior low speed performance, and reduced product quality, thus limiting the application of ac drives.

Fig. 3 shows the terminal voltage frequency spectrums and transfer function for a current regulated ac induction motor drive at rated load, 650 rpm, and without torque, flux, and encoder feedback. The spectrums are amplified to highlight the dominant sub and inter carrier harmonics present in the signals. Examination of the current feedback showed no sub or inter carrier harmonics. Expanding the frequency range reveals additional side lobes evenly space at multiples of the first side lobe. The frequencies of the side lobes are given by:

$$f_{+/-n} = f_e + \sum_{n=+/-1}^{\infty} 2nS \qquad (1)$$

The major components occur at f_e +/- 2S, where f_e is the excitation frequency (22.0 Hz) and S the slip frequency (0.35 Hz). The amplitude of the first side lobe is approximately 2.8 Vpk or 1% relative to the fundamental component. Of further significance, both components, as shown by the relative phase angles, are positive sequence signals. Although current components do not exist at these frequencies, the voltage components have an associated flux and serve to excite torque oscillations.

Fig. 4 shows a comparable motor condition but with an open loop V/F inverter. Here full load torque develops at S=0.53

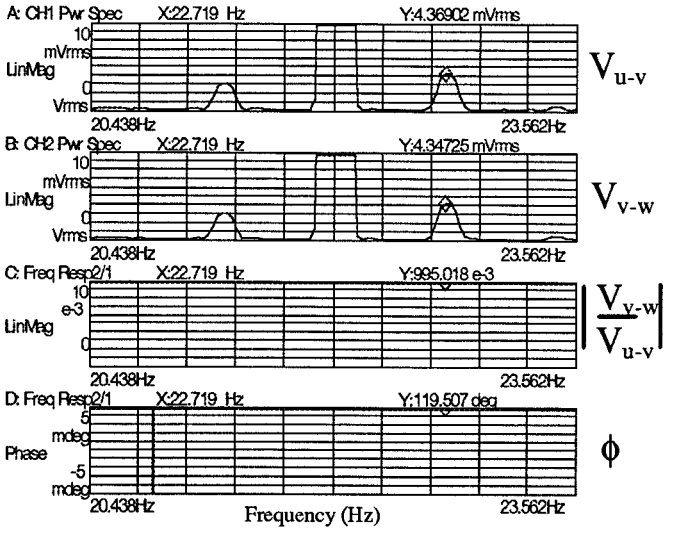

Fig. 3 Experimental results: Terminal voltage spectrum for a current regulated inverter induction motor.

Hz. Now the side lobes appear in the current spectrum at the multiples predicted by (1); torque oscillations result from the interaction of the current and flux components present. As Fig. 5 shows, these torque oscillations produce a speed variation at approximately 1 Hz. This speed fluctuation, introduced by the motor, acts as a disturbance and is depicted internal to the induction machine in Fig. 2.

III. PRACTICAL MOTOR DESIGN AND ITS EFFECT ON PERFORMANCE

FO control generally assumes the induction motor may be represented by a balanced set of sinusoidal windings, yielding linear inductances without magnetic losses. The resulting five parameter machine model provides a mathematically convenient model for the development of the slip and field relationships necessary for dynamic FO. However, the results presented above suggest these assumptions may oversimplify the motor model and prove inadequate on demanding applications.

Determining the cause for the machine behavior is difficult. Fig. 6 shows a simulation nearly representative of the conditions presented in Fig. 1. The motor model, however, is more complex than the traditional induction motor model. The model employed in the simulation is based on models reported in [7-9]. Although the simulation gives reasonable correlation to the experimental results of Fig. 1, the authors have observed deficiencies with the model and in this section will explore in detail the second and third order effects of practical machine design on drive performance.

A. Rotor Asymmetries and Abnormal Operation of Induction Machines

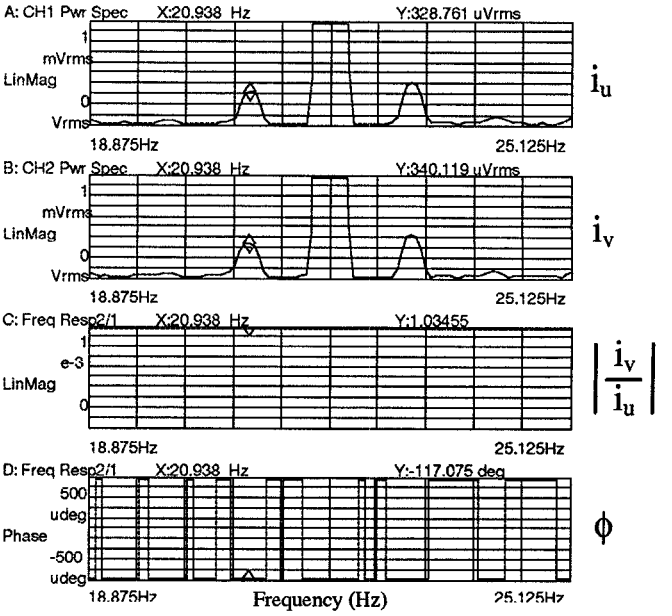

Fig. 4 Experimental results: Current feedback spectrums for a V/F motor drive.

Motor analysis and control traditionally assume ac motors to be modeled as lumped parameter electrical circuits; in fact, only the fundamental component is considered. This is especially true for a FO controller. The inclusion of motor space harmonics complicates the analysis and is neglected, while machine inductance asymmetry is assumed to be negligible. However, the winding distribution, stator/rotor slot combination, or rotor asymmetries caused by rotor electromagnetic variations can play a significant role and void implied assumptions inherent in the analysis and control.

Developing accurate models to predict second and third order effects observed on modern ac motor drives is an area of considerable interest. Given the frequency spectrum of the voltage (Fig. 3 current regulated) and current (Fig. 4 V/F

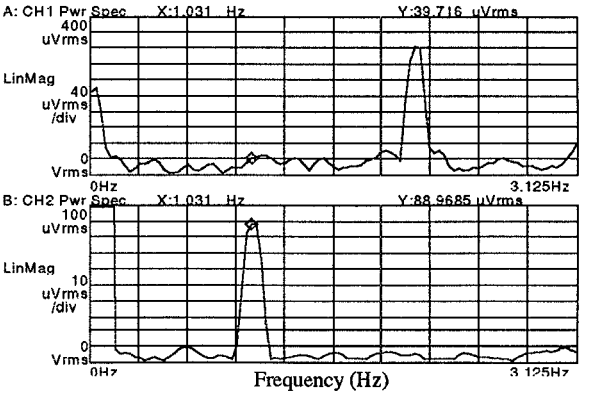

Fig. 5 Experimental results: Speed (lower) and current (upper) spectrums for Fig. 4.

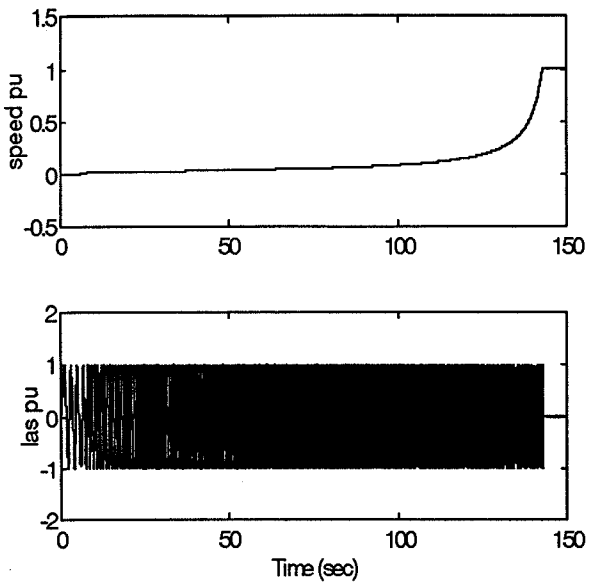

Fig. 6 Simulation results corresponding to Fig. 1.

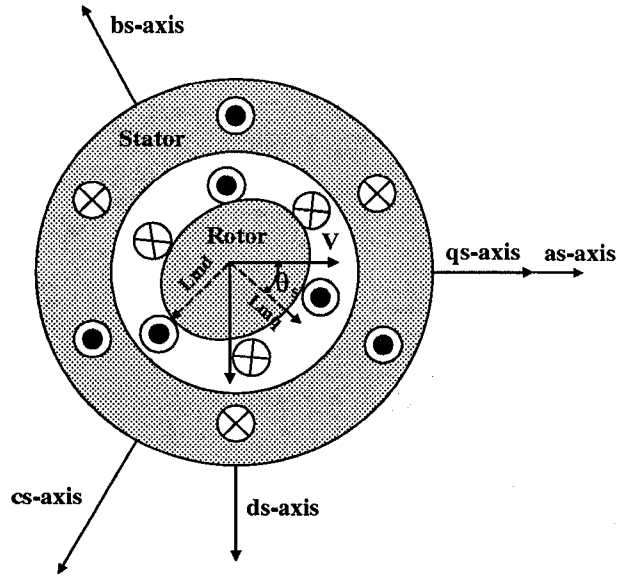

Fig. 7 Induction machine with rotor asymmetry.

open loop), one possible contributor to the type of behavior of Fig. 1 is the existence of a rotor asymmetry; possible origins of the asymmetry include residual magnetism, magnetic saturation, and magnetic or electrical distortion. Fig. 7 depicts this asymmetry and establishes an angle (θ_s) between the stator a-phase and the rotor q-axis or minimum inductance path of the rotor. A rotor asymmetry presents unique problems for high performance induction motor drives. Its existence may be established while field commissioning the drive system, whereupon corrective action may be taken to reduce its effects. To understand the effect of a rotor saliency on field commissioning, simulation studies were conducted; first an ideal machine is examined to demonstrate expected results, then the effects of a rotor saliency are incorporated to reveal the effect it has on the commissioning results.

Most high performance FO drive systems require a field commissioning procedure to identify critical machine and mechanical parameters [5]. Part of the procedure may require the repetitive acceleration/deceleration of the mechanical system. This is convenient when obtaining information about the motor including the magnetization characteristics. Fig. 8 shows simulation results for a FO control with position feedback intended to explain a procedure found to be successful in identifying the desired field current. The first or top trace displays the q-axis rotor flux (qr flux), the second trace the induction machine's electromagnetic torque (Te), the third trace the percent error between the desired field current and actual, and the fourth or bottom trace the speed of the machine (rpm). The procedure allows for the dynamic tuning of the field current. After commissioning, FO is established with a flux level providing sufficient voltage margin for current control and acceptable torque per amp.

The results of Fig. 8 correspond to a machine that is initially overexcited, thus the large error in the third trace. As the first and second traces clearly show, the machine is not FO during the first acceleration. After accelerating to a predetermined speed - approximately 80% of rated speed - the accelerating torque is set to zero. The machine is allowed to coast and the commissioning procedure collects data to select a more desirable field current. This is demonstrated in the third and fourth traces. Once a minimum speed is attained - approximately 10% of rated speed - accelerating torque is reapplied. Now notice the quality of the FO; the q-axis rotor flux is nulled, the torque constant, and a linear acceleration exists.

Fig. 9 shows simulation results for conditions similar to those presented in Fig. 8. The motor model, however, has been

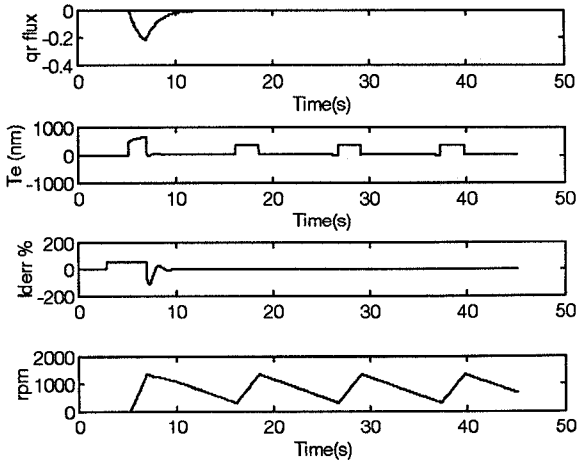

Fig. 8 Simulation results of over excited induction motor Id commissioning.

altered to reflect a rotor asymmetry; unequal magnetizing inductances exist in the q (L_q) and d (L_d) axes in this case. The rotor q-axis flux, torque, % error in d-axis current, and rpm are plotted. The saliency torque causes the machine to accelerate, even with the torque current (Iq) and slip set to zero. A braking torque is applied to decelerate the motor and allow the field commissioning procedure to proceed.

A simple explanation of the effect of rotor asymmetry within an induction motor is possible by referring to Fig. 7 and (2) [10]. V corresponds to the terminal voltage and P the number of magnetic poles. At stall and under flux up condition, the slip angle (θ_s) may be nulled, thus aligning the rotor with the ds-axis. When torque current is applied to the motor, the rotor develops the commanded slip frequency, and θ_s is created as the integral of the slip frequency. At the moment commanded speed is attained, the torque current and slip frequency are set to zero; however, the reluctance torque angle is not zero. In the case of Fig. 9, an accelerating torque develops. If left uncorrected, the machine's speed increases until either an over speed condition is sensed, whereupon a trip occurs (Fig. 6), or insufficient voltage margin exists and an over current trip occurs (Fig. 1).

$$T_e = \frac{3}{2}\frac{P}{2}\frac{1}{2}\left(\frac{1}{L_q}-\frac{1}{L_d}\right)V^2 \, Sin\,2\theta_s \qquad (2)$$

Another problem created by rotor asymmetries is steady state torque accuracy and transient FO. Fig. 10 shows transient and steady state simulation results of an induction motor in torque mode with a FO controller; FO (λ_{qr}=0) is maintained and speed deviation is minimal. However, Fig. 11 shows the results of the same control with a motor having an asymmetrical rotor. The torque oscillations at 2S induced by the rotor saliency are a disturbance, momentarily increasing and decreasing the machine's speed. If a position feedback device is employed, the machine's speed will drift as shown in Fig. 11. The machine flux pulsating at twice slip frequency increments the rotor position, and in combination with the slip angle forces the electrical frequency to track the disturbance. Clearly, the simple assumptions associated with FOC are invalid. In addition, the torque disturbance is low frequency and often within the bandwidth of demanding applications. Furthermore, the additional uncertainty in the instantaneous developed torque is not predicted by standard open loop torque observers. To reduce these effects, either the machine's slip or current must be modulated.

Experimental results were obtained for two modes of operation of FOC with position feedback on a 7.5 hp induction motor drive. Fig. 12 displays the spectrums of the terminal voltage and current feedback for a standard indirect FOC. Incorporating position feedback actually raises the subharmonic and inter carrier frequency content relative to Fig. 3; thus, the harmonic content present in the torque increases when position feedback is employed. Fig. 13 corresponds to the same operating conditions, but with a Model Reference Adaptive Control (MRAC) employed to adapt the FO slip gain (Ks in Fig. 2) [11]. Fig. 13 displays the spectrum of the slip gain. Notice the oscillation frequency corresponds to the difference between the fundamental of the voltage or current spectrums and their respective side bands (2S). Spectral analysis of the shaft torque indicates a 20% reduction in the 2S harmonic amplitude relative to Fig. 12. The MRAC reacts to the torque disturbance reflected in the terminal voltage by adjusting Ks. The effectiveness of the disturbance rejection depends on the bandwidth of the MRAC, which is limited by the voltage feedback characteristics.

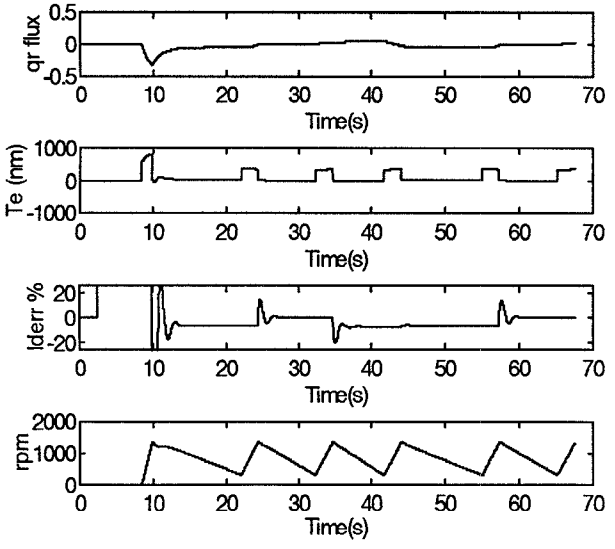

Fig. 9 Simulation results of over excited asymmetric induction motor Id commissioning 500 hp Id= 170 Apk Iq=100 Apk θ_s=0.

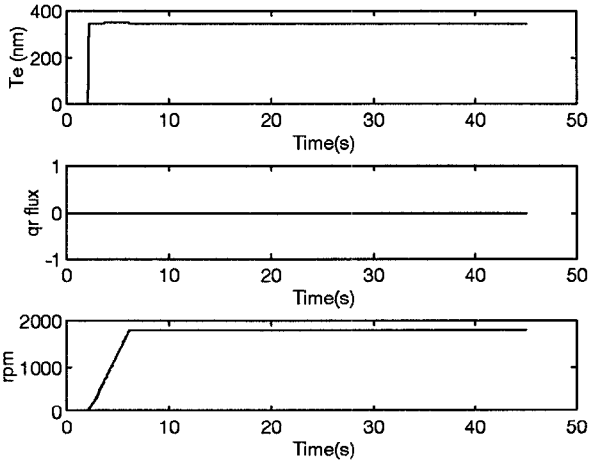

Fig. 10 Simulation results of FOC torque mode: Id= 170 Apk Iq=100 Apk Tload=Te*.

07803-4070-1/97/$10.00 (c) 1997 IEEE

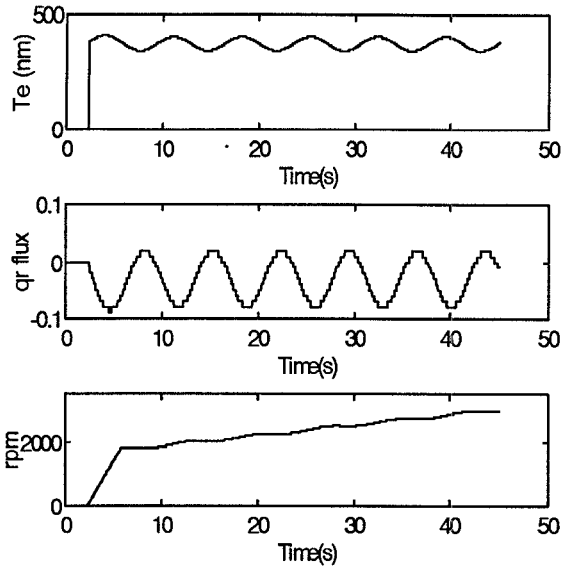

Fig. 11 Simulation results of asymmetrical machine: Id= 170 Apk Iq=100 Apk θ_s=0 Tload=Te*.

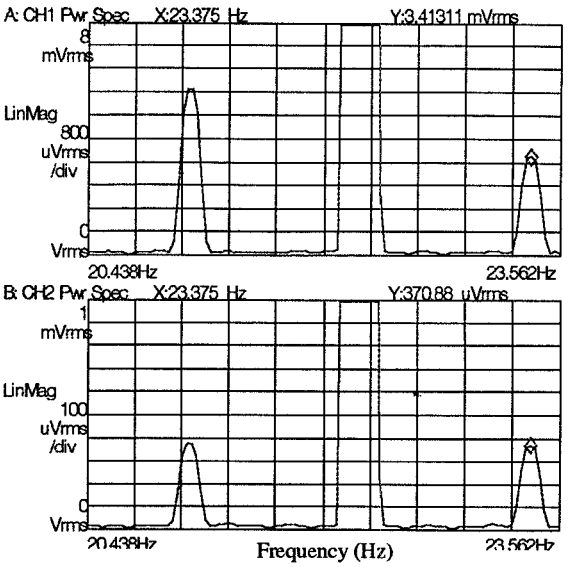

Fig. 12 Experimental results of FOC position feedback: voltage (top) and current (bottom) spectrums.

B. Machine Space Harmonics

Other possible contributors for the results displayed in Fig. 1 include: 1) mechanical misalignment of the position detector, 2) incorrect pulse counting, 3) control algorithm errors, 4) microprocessor performance limitations, 5) inter carrier voltage harmonics, and 6) space harmonics. This section examines the effects of space harmonics on motor drive performance. In this case, the space harmonics of the machine's windings produce average torque with synchronous speed at fractions of the fundamental frequency. Space harmonic contribute an accelerating or decelerating torque depending on a number of factors - slots per pole, coils per group, pitch, and throw.

The 400 hp motor (Fig. 1) was a 575 volt, 45 Hz, 6 pole machine with 90/74 stator-rotor slot ratio. Veinott calculated the winding factors and harmonic content for various coil groupings [1]. The dominate space harmonics for the 400 hp machine are the fifth and seventh winding factors. The relative weighting is 0.0312 and 0.0305 of the fundamental for the fifth and seventh space harmonics respectively. The fifth being a forward rotating subharmonic and the seventh a reverse rotating subharmonic.

A simulation was developed to include the effects of space harmonics [3,7-9]. Fig. 14 displays typical results. In the results shown, the fifth and seventh space harmonics are included with the weighting relative to the fundamental as indicated above. Although the simulation employs variable frequency sine waves, the electromagnetic torque contains high frequency components as a result of the space harmonics. The fifth and seventh space harmonics combine to provide an accelerating torque. By applying a braking torque similar to Fig. 9, the commissioning procedure converges without difficulty. Field data has shown up to 10% of rated torque necessary to hold speed at no-load, indicating a significant torque offset from the machine's space harmonics.

IV. CONTROL STRATEGIES TO REDUCE ZERO SLIP TORQUE INDUCED BY ROTOR ASYMMETRIES

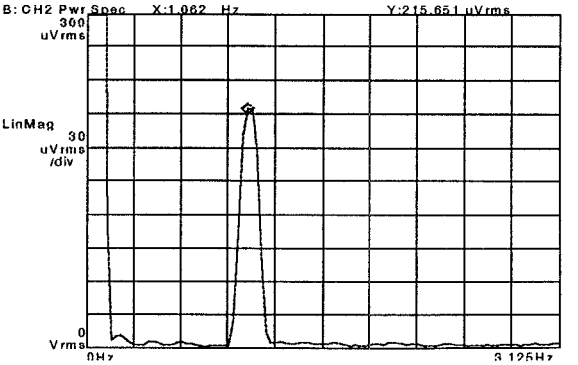

Fig. 13 Spectrum of MRAC Ks (Fig. 2) full load. Frequency (Hz)

The degree to which machine design may be altered to improve drive performance is limited. Reducing the steady state torque contributed by the space harmonics of the stator winding is one area for investigation and reexamining the stator - rotor slot combinations to reduce rotor asymmetries is another. However, the application of existing machine designs requires these problems be addressed through control. One approach, suggested by the results above, is to employ a MRAC to on-line adaptively modulate the slip gain to reduce the torque pulsations induced by rotor irregularities and space harmonics. To improve commissioning convergence and prevent the need for counter acting torque at no-load, other approaches are possible.

One approach is to simply apply a braking torque following acceleration. Fig. 9 is a simulation demonstrating this concept. The field current error is amplified to clearly show the dynamic effects of rotor saliency and the convergence of the field current tuning procedure. Unlike the ideal machine of Fig. 8, the machine with rotor saliency fails to null the q-axis rotor flux; the developed torque contains a low frequency oscillation, and the field current displays a considerable transient while braking. However, the field commissioning procedure did converge and determine the correct field current. Simulations and experience has confirmed it is desirable to minimize the reluctance torque at the beginning of the deceleration period of the commissioning procedure and at no load operation.

If the nonzero torque condition is caused by rotor asymmetry, at least two options are available to enhance convergence of the field commissioning procedure and no load operation of the drive system. Each method affects the dynamics of the field commissioning procedure and the transition to no load operation. The first solution, θ_s reset with ramp control, forces the torque to become zero by resetting θ_s to zero at the instant the torque command becomes zero. Fig. 15 displays simulation results of this approach and Fig. 16 shows a block diagram of the control.

Once the speed set point is reached, the torque current and slip frequency are set to zero. Simultaneously, θ_s is reset to zero through a ramp with an adjustable rate, and in the case of the field commissioning procedure the q-axis flux regulator is activated. The regenerative torque developed is a function of the rate of the θ_s reset. Following reset, the speed slowly decreases and the q-axis regulator controls the flux of the machine through the d-axis current. In contrast to the results of Fig. 9, the machine does not require a braking torque; the machine now coasts as before and the q-axis regulator establishes the d-axis current with a very small error.

Another method applies a braking torque to the machine to enhance deceleration - Fig. 17. As described above (Fig. 9), this approach has the disadvantage of requiring the development of slip while braking. The resulting pole slipping presents a disturbance to the field current commissioning procedure and may require more accel/decel cycles for a reasonable estimate of the field current.

Fig. 18 shows experimental results of the braking approach applied to the 400 hp induction machine of Fig. 1. The velocity and torque current are displayed over a complete duty cycle of the portion of the commissioning procedure establishing the field current. After reaching the desired speed (7 sec), the torque current and slip are set to hold speed, but the motor continues to creep (12 sec). The control detects the acceleration and commands sufficient braking torque to decrease the machine's speed (18 sec). Once the low speed limit is reached, the torque command changes to accelerating and the speed ramps to the desired speed. After reapplying braking torque, the commissioning procedure converges, terminates the commissioning procedure, and brakes the motor.

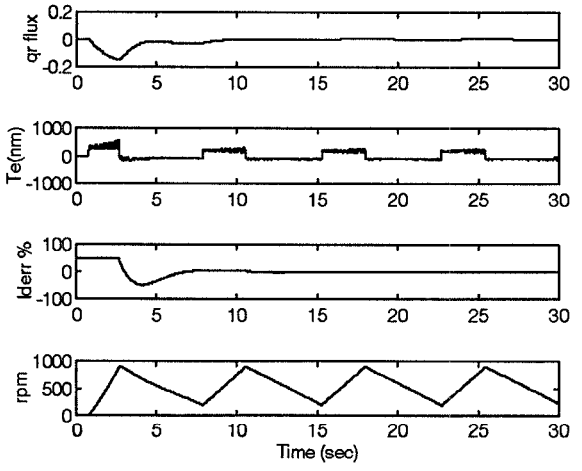

Fig. 14 Simulation results of over excited induction motor Id commissioning: 400 hp 5th and 7th space harmonics Id= 82 Apk Iq=50 Apk braking torque.

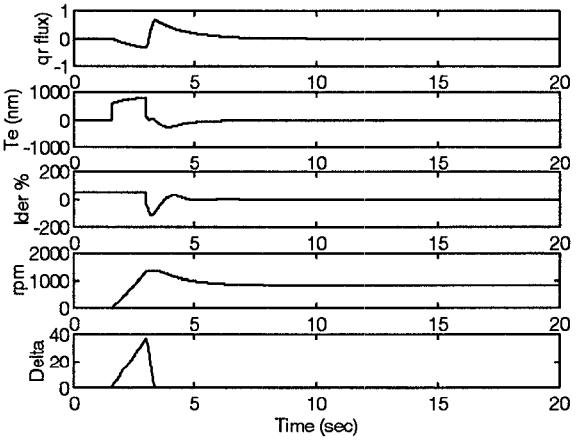

Fig. 15 Simulation results of the θ_s reset with ramp control

07803-4070-1/97/$10.00 (c) 1997 IEEE

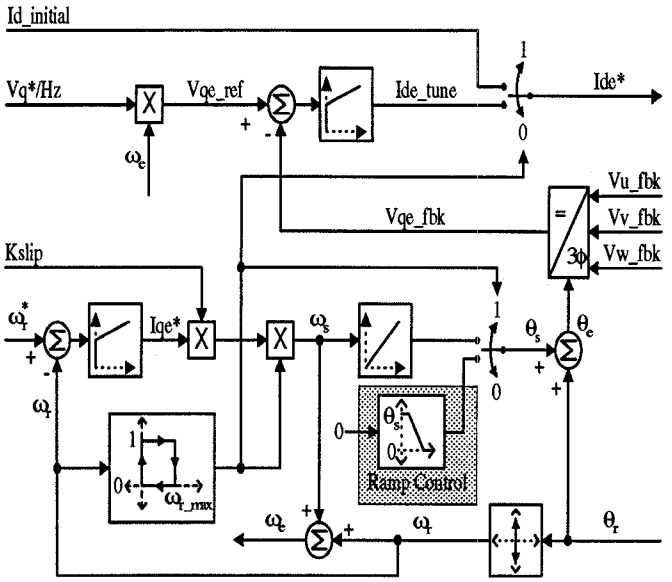

Fig. 16 θ_s reset ramp control block diagram.

V. CONCLUSIONS

Experimental results were presented demonstrating abnormal operation of induction machines. State of the art field commissioning procedures can fail to converge due to motor irregularities. A failure may be exhibited by an uncharacteristic over speed condition and an ability to accelerate under flux up. Possible causes were discussed, and two induced by the machine were investigated: 1) induction motor rotor asymmetries due to asymmetrical rotor bar distribution, magnetic saturation, or magnetic distortion, 2) induction motor space harmonics. Experimental data reveals sub-harmonics in the voltage and current spectrums at frequencies corresponding to rotor asymmetries. Simulations including dominant machine space harmonics demonstrate their contribution to average torque and torque oscillations.

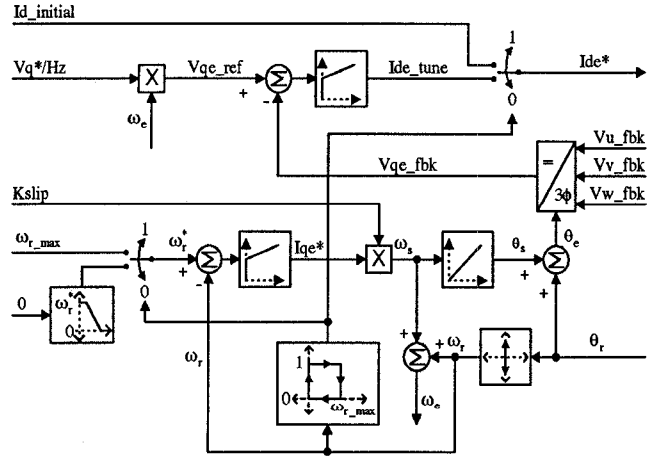

Fig. 17 Control block diagram of the braking torque method

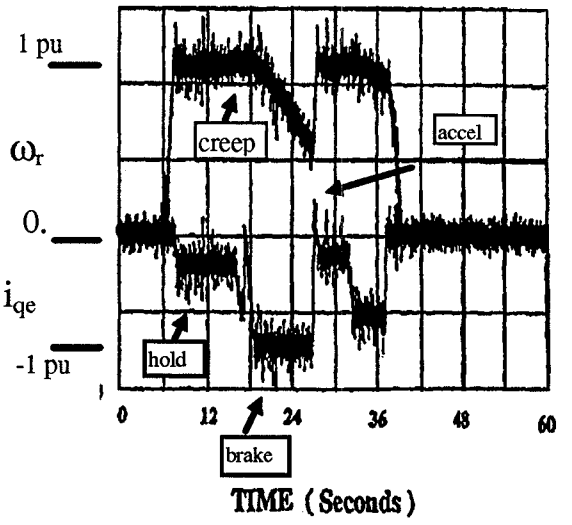

Fig. 18 Experimental results of applying braking torque control: speed (upper) 1 pu = 580 rpm and Iq (lower) 1 pu = 73 Apk.

Low frequency oscillations observed in the machine's velocity confirm the presence of low frequency torque components. Control procedures to reduce the disturbances created by rotor asymmetries were presented. Simulation and experimental results show the dynamic and steady state improvement these procedures provide.

VI. REFERENCES

[I] C. Veinott, "Theory and Design of Small Induction Motors," McGraw-Hill Book Company, Inc., 1959.

[2] G. L. Skibinski, "Skewing Effects & Design Considerations of the 1250 HP AC Motor," Internal Report Allen-Bradley Co., 1994.

[3] H. A. Toliyat and T. A. Lipo, "Transient Analysis of Cage Induction Machines Under Stator, Rotor Bar and End Ring Faults," IEEE-PES Summer Meeting, San Francisco, CA, July 24-28, 1994.

[4] Emil Levi, Matija Sokola, Aldo Boglietti, and Michele Pastorelli, "Iron Loss in Rotor-Flux-Oriented Induction Machines: Identification, Assessment of Detuning, and Compensation", IEEE Trans. on Power Electronics, Vol. 11, No. 5, Sept. 1996, pp. 698-709.

[5] Russel J. Kerkman, Jerry D. Thunes, Timothy M. Rowan, and David W. Schlegel, "A Frequency-Based Determination of Transient Inductance and Rotor Resistance for Field Commissioning Purposes," IEEE Trans. on Industry Applications, Vol. 32, No. 3, May/June 1996, pp. 577-584.

[6] T. Mizuno, J. Takayama, T. Ichioka, M. Terashima, "Decoupling Control Method of Induction Motors Taking Stator Core Loss into Consideration," IPEC (Tokyo, Japan), 1990, pp. 69-74.

[7] H. A. Toliyat, M. S. Arefeen, and A. G. Parlos, "A Method for Dynamic Simulation and Detection of Air-Gap

Eccentricity in Induction Machines," IEEE IAS Annual Meeting, Orlando, Florida, Oct. 8-12, 1995, pp. 629-636.
[8] H. R. Fudeh and C. M. Ong, "Modeling and Analysis of Induction Mcahines containing Space Harmonics Part 1: Modeling and Transformation," IEEE/PES 1983 Winter Meeting, New York, N.Y., Jan. 30 - Feb. 4, 83 WM 192-2.
[9] H. R. Fudeh and C. M. Ong, "Modeling and Analysis of Induction Machines containing Space Harmonics Part 2: Analysis of Synchronous and Asynchronous Actions," IEEE/PES 1983 Winter Meeting, New York, N.Y., Jan. 30 - Feb. 4, 83 WM 193-0.
[10] P. C. Krause, "Analysis of Electric Machinery," McGraw Hill Book Company, 1986.
[11] Timothy M. Rowan, Russel J. Kerkman, and David Leggate, "A Simple On-Line Adaption for Indirect Field Orientation of an Induction Machine," IEEE Trans. on Industry Applications, Vol. 27, No. 4, July/August 1991, pp. 720-727.

07803-4070-1/97/$10.00 (c) 1997 IEEE